Acoustic Emission from Breaking a Bamboo Chopstick

Sun-Ting Tsai, Li-Min Wang, Panpan Huang,* Zhengning Yang,† Chin-De Chang, and Tzay-Ming Hong‡
Department of Physics, National Tsing Hua University, Hsinchu 30013, Taiwan, Republic of China
(Received 3 September 2015; published 19 January 2016)

The acoustic emission from breaking a bamboo chopstick or a bundle of spaghetti is found to exhibit similar behavior as the famous seismic laws of Gutenberg and Richter, Omori, and Båth. By the use of a force-sensing detector, we establish a positive correlation between the statistics of sound intensity and the magnitude of a tremor. We also manage to derive these laws analytically without invoking the concept of a phase transition, self-organized criticality, or fractal. Our model is deterministic and relies on the existence of a structured cross section, either fibrous or layered. This success at explaining the power-law behavior supports the proposal that geometry is sometimes more important than mechanics.

DOI: 10.1103/PhysRevLett.116.035501

Fracture [1] is a complex phenomenon with many interesting properties, such as crack propagation [2], breakdown [3], and self-affine fractals in the crack surface morphology [4]. This kind of study started in seismology and attracted the attention of physicists and material scientists. Crackling noise [5,6] in the acoustic emission from a fracturing wood plate [7], paper [8,9], rock [10], concrete [11], and charcoal [12] has been found to exhibit similar statistical properties as an earthquake [13,14]. On the other hand, the slow growth of a single crack in a fibrous sheet has been studied by the lattice model [9] which incorporates thermodynamics to describe the temperature dependence. To understand the failure process, the fiber bundle model [15] has also been extended [16] by introducing time-dependent damage accumulation of fibers to capture the stochastic nature of fracture.

In contrast to 2D and 3D samples in previous fracture experiments, we shall adopt the 1D-like chopstick because it rarely fractures in multiple places at the same time, which makes the interpretation of data easier. Chopsticks are easily accessible because they are indispensable implements for most Asian families and carry special cultural meaning [17] in Chinese tradition. They are usually made by bamboo in Taiwan and China. Bamboo exhibits a fibrous cross section. Its excellent compressive strength, endowed from the vascular bundles scattered throughout the stem in the cross section instead of in a cylindrical arrangement, enables us to collect about 400 crackling sounds from breaking one chopstick, as opposed to just one sound from a chalk or twig.

Our main sample is the cheap and omnipresent bamboo chopstick of diameter 0.67 cm and length 20.5 cm. Sticks are also taken directly from the bamboo tree to make sure our conclusions are independent of the length, freshness, and processing to turn them into chopsticks. A bundle of spaghetti [18] is also used to check the generality of our model because it shares a similar cross section as bamboo (see Fig. 1). The fracture machine in Fig. 2 is placed inside a soundproof chamber with a foam rubber plank on the interior to avoid echo. A Sony ECM166BC microphone that is connected to a Sony ICD-PX333 recorder picks up the fracture sound. By tightening the screw, the movable metal block was driven and compressed the chopstick. The bolted plate is to secure the bent chopstick from slipping and flying off. The chopstick was flipped into a horizontal position as soon as it became bent to prevent fracturing near the plate edge. A crackling sound was recorded at a sample rate of 44 100 points per second in 16-bit precision. The amplitude was measured in computer units and the maximum amplitude was $A_{\max} = 2^{15} - 1$. The gain of the sound card was constant and samples were positioned at a distance of 5 cm from the microphone. We kept the process of fracture at a steady velocity of about 200 s per chopstick.

The average amplitude of the background noise was 3×10^{-3} as normalized by $A_{\max}$, and thrice this amount was set as the noise threshold. The *c*-code algorithm automatically integrated the sound intensity every 200/44 100 s. When the value exceeded the background noise, the beginning of a new pulse was marked, as in Fig. 2(c). Whenever a dilemma arose with distinguishing a long pulse from two overlapping pulses as in Fig. 2(d), we resorted

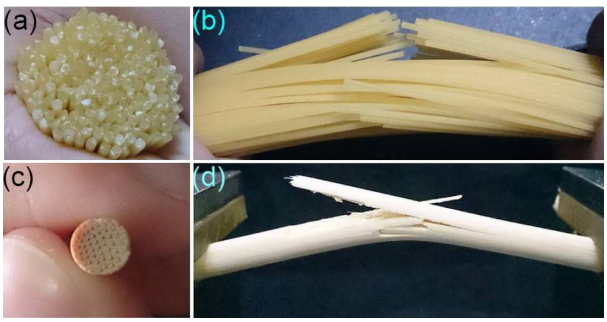

FIG. 1. Panels (a) and (c) show the similar structure in cross section between a bundle of spaghetti and a bamboo chopstick. Panels (b) and (d) are the side view during fracture.

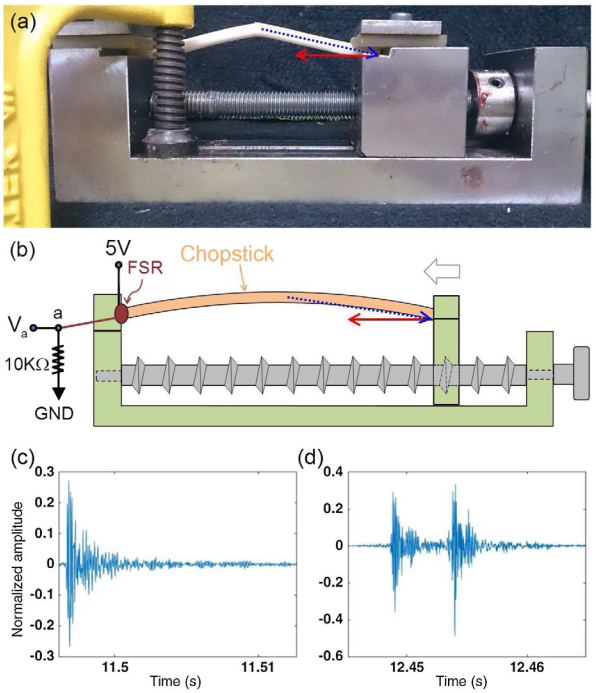

FIG. 2. Panels (a) and (b) show the fracture machine. FSR is the acronym for force-sensing resistor, and GND is the shorthand for ground. The blue dotted arrow represents the arm of force, and the red solid arrow represents the force exerted on one end of the chopstick. Panel (c) shows a typical sound pulse, and (d) shows an example when one long pulse or two overlapping pulses need to be distinguished.

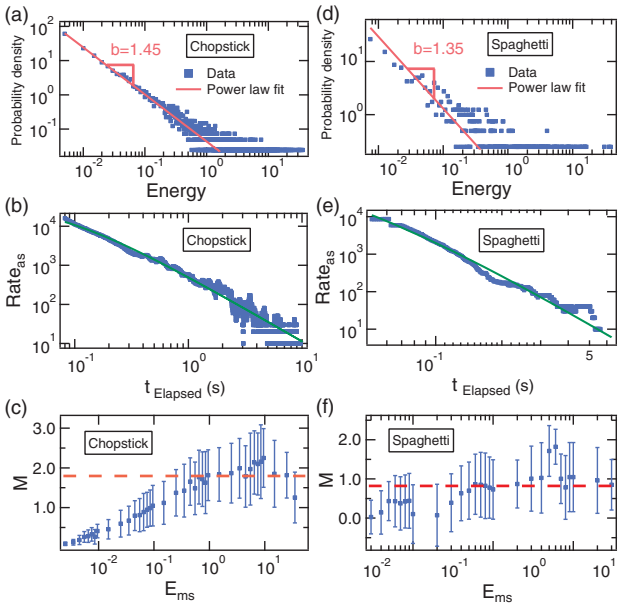

FIG. 3. Panels (a)–(c) are for the crackling sound from the bamboo chopstick, while (d)–(f) are from a bundle of spaghetti. They mimic the Gutenberg-Richter law, the Omori law, and the Båth law for earthquakes. The power-law exponent in (a) and (d) is determined to be 1.45 and 1.35. The exponent and shift in (b) and (e) are ($p = 1.68$, $c = 0.07$) and (3.53, 0.027). The relative magnitude M in panels (c) and (f) is defined as the average of $\log(E_{ms}) - \log(E_{la})$, where E_{ms} and E_{la} denote, respectively, the energy of the main shock and its largest aftershock. Error bars represent standard deviations.

to a smaller time step to examine the intermediate area by including just six amplitude peaks of the oscillation within the pulse(s). Since this value is expected to decrease as a pulse fades, a sudden switch to an increasing function indicates the beginning of a second pulse.

After squaring the amplitude and integrating over the duration time to obtain the energy for each sound pulse, we grouped the data into a histogram of probability function versus pulse energy. A full logarithm was then taken in Figs. 3(a) and 3(d) to reveal a good alignment, indicative of a power law: $P(E) \sim 1/E^b$ that is reminiscent of the Gutenberg-Richter law [19]. The exponent b for the chopstick is about 1.45 by the use of the maximum likelihood estimation (MLE). When we sliced the chopstick horizontally into two halves, the power law persisted but the upper (lower) hemisphere became $b = 1.48$ (1.40). The empirical value of b for an earthquake is commonly close to 1.0 in seismically active regions, but may vary in the range of from 0.5 to 2 depending on the source environment of the region [20].

The aftershock rate in Figs. 3(b) and 3(e) was defined as the number of aftershocks divided by the time window of 100 ms, against the elapsed time $t_{elapsed}$. And aftershocks referred to the sound pulses on the time series between two local maxima in pulse energy, i.e., the main shocks. Since the number of local maxima roughly matches that of vascular bundles, we believe the fracture of each bundle gives rise to one main shock and a few aftershocks. A shifted power law, $\text{rate} = k/(c + t_{\text{elapsed}})^p$, where k and c are constants, similar to the Omori law [21] was deduced. The exponent in Fig. 3(b) was determined by MLE to be $p = 1.68$, slightly larger than the region of 0.75–1.5 set for earthquakes. Finally, after an initial dip in Figs. 3(c) and 3(f) that is known to exist in real data [22,23], the M value became independent of the main-shock magnitude and saturated at 1.7–1.8 in Fig. 3(c)—somewhat higher than 1.1–1.2 for the Båth law [24].

In spite of a multitude of workers who have compared the acoustic emission from laboratory material to the shock energy of earthquakes, the reasonable assumption that these two energies are correlated was rarely proven. We thus decided to affix a force-sensing resistor (FSR) to the end of the chopstick in Fig. 2 and compared the timing and statistical behavior of the discrete events of tremor and acoustic emission. When the reaction force by the chopstick increased, the resistance of FSR (Interlink Electronics FSR402) decreased from an initial value higher than 10 M(Ω) and generated a nonzero voltage V_a. An Arduino UNO board then collected the measurement of V_a at a sample rate of 100 points per second.

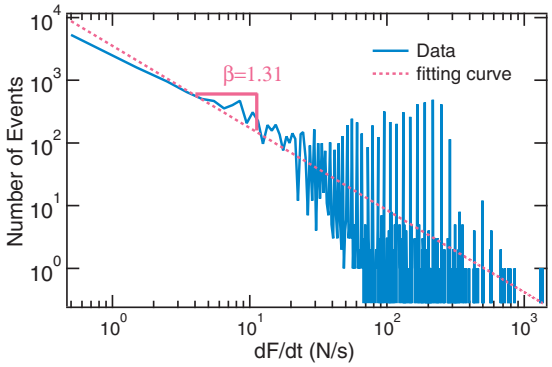

FIG. 4. Full-log plot of the number of events versus the magnitude of force change picked up by FSR. Data were fit to a power law (the red dotted line) with an exponent roughly equal to that of the crackling sound in Fig. 3(a).

Any fracture is expected to cause a sudden drop in reaction force against the FSR, but not necessarily accompanied by a detectable sound. Therefore, there is no one-to-one correspondence between these two events, with there being more tremors than sounds. Any discussion of their correlation has to be effectuated through comparing their statistics. We thus grouped the nonzero values of the time derivative of force dF/dt into a histogram. A power-law distribution $P(dF/dt) \sim 1/(dF/dt)^{\beta}$ emerged with $\beta = 1.31$ in Fig. 4. This is to be contrasted to Fig. 3(a). The fact that both figures exhibit power-law behavior with a similar exponent and a valid range of parameter confirms a positive correlation between energies of the quake and the crackling sound. The chaotic distribution when dF/dt exceeds 10 N/s was caused by the drop of sensitivity in FSR when the force change is larger than 10 N. Limited by the sensitivity of FSR, we believe the number of small events it picked up was underestimated, which probably explains why $\beta = 1.31$ is slightly smaller than $b = 1.45$ in Fig. 3(a).

A minimal model will be presented to explain qualitatively why the major seismic laws should appear in the humble bamboo chopstick. In contrast to numerical simulations that are popular for the study of fracture in disordered media [25], we believe analytical derivations can provide more insight. Since the Gutenberg-Richter and Båth laws concern only the energetics, they will be tackled separately from the Omori law, which requires dynamics. For simplicity, we consider only a rectangular cross section, but other shapes can be easily generalized.

Two features in Fig. 5 merit attention. First is the progressive shortening of effective length l_n—the length of beam neutral axis that is actually bent. Second, the end segments of the chopstick remain straight because they are thicker and less susceptible to bending. To nail down the relevant factors and enable analytic solutions, we will focus on the bending energy in the static beam equation, which includes tensional and compressional stresses in the cross section external and internal to the beam neutral axis, respectively:

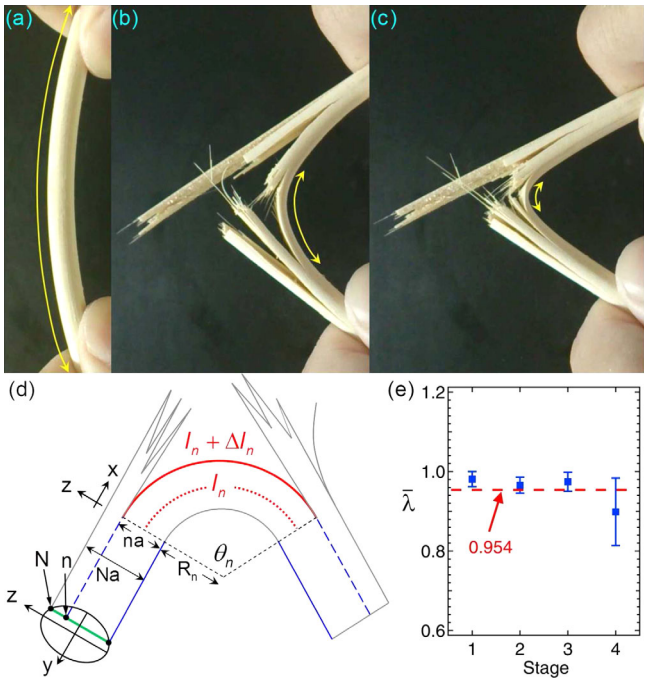

FIG. 5. Yellow double-arrowed lines in panels (a)–(c) highlight the shortening of the effective length. In panel (d), the fiber on the nth layer is stretched and on the verge of fracturing. The R_n represents its radius of curvature, and θ_n the angle spanned by the bent section (in the dotted red line). Note the end segments (in the blue dashed line) remain straight, resembling the V-shape configuration in Ref. [27]. In panel (e), the reduction ratio of the effective length is determined for different time stages.

$$E_{\mathrm{tot}} \approx \int_0^{l_n} dx \int dy \frac{K_B}{2} \left(\frac{1}{R_n}\right)^2, \tag{1}$$

where $K_B \sim Y(na)^3$ and Y denotes the Young's modulus. As exemplified by Figs. 5(b) and 5(c), the fractured segment of bamboo remains rather straight, which demonstrates that the plastic region preceding fracture is very narrow and the elastic form of Eq. (1) can be extended to large strains. As fracture proceeds in the tensional region, n decreases and l_n is shortened progressively as evidenced by Figs. 5(a)–5(c) and our YouTube clip [26].

Geometric relations can be written down from Fig. 5(d)

$$\begin{aligned} l_n + \Delta l_n &= (R_n + na)\theta_n, \\ l_n &= \left(R_n + \frac{na}{2}\right)\theta_n. \end{aligned} \tag{2}$$

Subtracting them gives

$$\frac{na}{2}\theta_n = \Delta l_n = \varepsilon l_n, \tag{3}$$

where the threshold strain for fracture, $\varepsilon \equiv \Delta l_n / l_n$, is a material property. Simple algebra gives

$$\frac{\Delta l_n}{l_n} = \frac{\frac{na}{2}}{R_n + \frac{na}{2}} \approx \frac{na}{2R_n}, \tag{4}$$

since $R_n \gg na$. For a rectangular cross section, the y integration simply gives a constant and the energy stored in the nth layer is roughly

$$E_n \approx E_{\text{tot}}/n = \frac{1}{n} l_n \frac{Yna}{2} \varepsilon^2 \propto l_n. \tag{5}$$

Since the stress is larger away from the beam neutral axis, the equipartition approximation of $E_n/E_{\text{tot}} \approx 1/n$ is an underestimation.

The fracture process was divided into four time stages in Fig. 5(e). If there are 400 pulses, take the ratio of l_{301}/l_{400}, where l_{301} and l_{400} represent the effective length measured upon the 100th and the first pulses, and define it as $\bar{\lambda}^{100}$ where $\bar{\lambda}$ is the mean value. Figure 5(e) shows that $\bar{\lambda}$ is roughly constant. The deviation of the $\bar{\lambda}$ value and a large error bar in the final stage is likely caused by the uncertainty in the pulse number because the crackling sound becomes very feeble. From these observations, the effective length can be assumed to obey

$$l_n = l\lambda^{N-n}, \tag{6}$$

where l denotes the initial length and $\lambda < 1$ is a material property. A similar concept has been used to explain the power-law behavior of the crackling sound from a crumpled thin sheet [28].

The total number of crackling sounds equals

$$\sum_n \approx \int dn = \int \frac{dn}{dE_n} dE_n. \tag{7}$$

Dividing both sides by $\sum$, we get unity on the left side to conserve the probability while the occurrence rate can be identified as $P(E_n) \propto dn/dE_n \sim 1/E_n$ by using Eqs. (5) and (6). This reproduces the power law in Fig. 3(a). If we increase the ratio $E_n/E_{\text{tot}} = 1/n$, the exponent will become larger and closer to the empirical value $b = 1.45$ in Fig. 3(a). When the rectangular cross section is changed to, say, the southern hemisphere of a horizontally halved chopstick, the width and fiber number of each layer decrease as the fracture propagates downward from the top. Since the top layers emit stronger pulses according to Eqs. (5) and (6), there is now a predominance of loud sound rather than weak sound. And we expect Fig. 3(a) to level off and give a smaller b. This is consistent with our observation.

To derive the Omori law, we need the time interval between successive aftershocks to calculate the elapsed time in Fig. 3(b). By assuming a constant angular acceleration during this short interval, we can estimate this time, Δt_n for the torque to render a displacement of $\Delta\theta_n$:

$$\Delta\theta_n = \theta_{n-1} - \theta_n = \frac{1}{2}(Fl \sin\theta_n/I)(\Delta t_n)^2, \tag{8}$$

where I denotes the moment of inertia. Since the bending force F comes from far ends of the chopstick, the arm of force equals l, not l_n. The $\sin\theta_n$ factor is due to the fact that the force is not perpendicular to its arm. Finally, since θ_n is mostly small, $\sin\theta_n \approx \theta_n$. As $n \gg 1$, we can replace $\Delta\theta_n$ by $d\theta_n/dn$ and obtain from Eq. (8):

$$(\Delta t_n)^2 \propto \ln\lambda + \frac{1}{n} \tag{9}$$

by the use of Eqs. (4) and (6). This shows that the time interval to the next aftershock increases with the number of broken fibers $N - n$. A simple way of understanding this slowdown in braking is that the tensional stress external to the beam neutral axis is lessened as the chopstick gets thinner. Consequently, it takes a larger angular displacement and longer time to reach the threshold strain for fracture. The aftershock rate can be calculated by dividing the number of aftershocks, $n_{\text{ms}} - n$, by the time lapse from their corresponding main shock, $\Delta t_{n_{\text{ms}}-1} + \Delta t_{n_{\text{ms}}-2} + \cdots + \Delta t_n$, where $n_{\text{ms}} \gg 1$ labels any one of the main shocks. Since the maximum number of aftershocks, $n_{\text{ms}} - n$, is in the ballpark of 8, we can Taylor expand the denominator by the small parameter, $1 - (n/n_{\text{ms}}) \ll 1$ and obtain

$$\text{rate} = \frac{n_{\text{ms}} - n}{\sum_n^{n_{\text{ms}}-1} \Delta t_n} \approx \frac{n_{\text{ms}}}{D' + (D''/2)[1 - (n/n_{\text{ms}})]}, \tag{10}$$

where the D' and D'' denotes the first and second derivative. Since $n_{\text{ms}} - n$ is roughly a measure of time, Eq. (10) reproduces the shift and power law of Fig. 3(b).

Since $E_n/E_{n-1} \sim 1/\lambda$ is independent of the value of n and insensitive to the approximation of $E_n/E_{\text{tot}} = 1/n$, the Båth law is naturally guaranteed.

In conclusion, we establish a complete parallel between the crackling noise of a common bamboo chopstick and a bundle of spaghetti and the fundamental seismic laws. The statistics of these acoustic events is shown to correlate with that of tremor. The fitting function and corresponding parameters are determined by the rigorous statistical method of the Akaike information criterion [28,29] and MLE. We succeed at deriving these laws analytically without invoking the concept of phase transition [5], self-organized criticality [30,31], or fractal [14]. Our models are based mainly on a structured cross section, which can be either fibrous or layered. This shift of emphasis from mechanics to geometry to explain the power-law behavior is in conformance with the proposal of Ref. [32].

We gratefully acknowledge funding from MoST in Taiwan, technical support by Jing-Ren Tsai, and the hospitality of the Physics Division of NCTS in Hsinchu.

*Present address: Department of Physics and Astronomy, Northwestern University, 2145 Sheridan Road, Evanston, Illinois 60208, USA.

[†]Present address: Department of Physics, University of Science and Technology of China, Hefei, Anhui 230026, China.
[‡]ming@phys.nthu.edu.tw

[1] J. Fineberg, S. P. Gross, M. Marder, and H. L. Swinney, Phys. Rev. B **45**, 5146 (1992); M. Marder, Nature (London) **381**, 275 (1996); A. Omeltchenko, J. Yu, R. K. Kalia, and P. Vashishta, Phys. Rev. Lett. **78**, 2148 (1997); M. J. Alava, P. K. V. V. Nukala, and S. Zapperi, Adv. Phys. **55**, 349 (2006).

[2] J. S. Langer, Phys. Rev. Lett. **70**, 3592 (1993); J. M. Carison and B. E. Shaw, Rev. Mod. Phys. **66**, 657 (1994); M. Marder, Phys. Rev. Lett. **74**, 4547 (1995); E. Sharon, S. P. Gross, and J. Fineberg, *ibid.* **76**, 2117 (1996); D. Bonn, H. Kellay, M. Prochnow, L. Ben-Djemiaa, and J. Meunier, Science **280**, 265 (1998); F. F. Abraham, Adv. Phys. **52**, 727 (2003).

[3] S. Zapperi, P. Ray, H. E. Stanley, and A. Vespignani, Phys. Rev. E **59**, 5049 (1999).

[4] A. S. Balankin, Eng. Fract. Mech. **57**, 135 (1997); A. Yavari, S. Sarkani, and E. T. Moyer, Jr., Int. J. Fract. **114**, 1 (2002); L. Goehring, A. Nakahara, T. Dutta, S. Kitsunezaki, and S. Tarafdar, *Desiccation Cracks and their Patterns: Formation and Modeling in Science and Nature* (John Wiley & Sons, Weinheim, 2015).

[5] J. P. Sethna, K. A. Dahmen, and C. R. Myers, Nature (London) **410**, 242 (2001); J. P. Sethna, *Entropy, Order Parameters, and Complexity* (Oxford University Press, Oxford, 2010).

[6] E. K. H. Salje and K. A. Dahmen, Annu. Rev. Condens. Matter Phys. **5**, 233 (2014).

[7] A. Garcimartin, A. Guarino, L. Bellon, and S. Ciliberto, Phys. Rev. Lett. **79**, 3202 (1997); A. Guarino, A. Garcimartin, and S. Ciliberto, Eur. Phys. J. B **6**, 13 (1998).

[8] L. I. Salminen, A. I. Tolvanen, and M. J. Alava, Phys. Rev. Lett. **89**, 185503 (2002).

[9] S. Santucci, L. Vanel, and S. Ciliberto, Phys. Rev. Lett. **93**, 095505 (2004); N. Yoshioka, F. Kun, and N. Ito, *ibid.* **101**, 145502 (2008).

[10] T. Hirata, J. Geophys. Res. **92**, 6215 (1987); P. Diodati, F. Marchesoni, and S. Piazza, Phys. Rev. Lett. **67**, 2239 (1991).

[11] A. Petri, G. Paparo, A. Vespignani, A. Alippi, and M. Costantini, Phys. Rev. Lett. **73**, 3423 (1994).

[12] H. V. Ribeiro, L. S. Costa, L. G. A. Alves, P. A. Santoro, S. Picoli, E. K. Lenzi, and R. S. Mendes, Phys. Rev. Lett. **115**, 025503 (2015).

[13] J. R. Rice, in *Physics of the Earth's Interior, Proceedings of the International School of Physics "Enico Fermi," Course 78, 1979*, edited by A. M. Dziewonski and E. Boschi (Italian Physical Society/North Holland, Amsterdam, 1980), pp. 555–649; D. L. Wells and K. J. Coppersmith, Bull. Seismol. Soc. Am. **84**, 974 (1994); E. L. Olson and R. M. Allen, Nature (London) **438**, 212 (2005); J. Faillettaz, M. Funk, and D. Sornette, Science **12**, 2977 (2012).

[14] D. L. Turcotte, *Fractals and Chaos in Geology and Geophysics*, 2nd ed. (Cambridge University Press, New York, 1997).

[15] J. V. Andersen, D. Sornette, and K. T. Leung, Phys. Rev. Lett. **78**, 2140 (1997); R. C. Hidalgo, C. U. Grosse, F. Kun, H. W. Reinhardt, and H. J. Herrmann, *ibid.* **89**, 205501 (2002).

[16] F. Kun, Z. Halasz, J. S. Andrade, Jr., and H. J. Herrmann, J. Stat. Mech. (2009) P01021.

[17] https://en.wikipedia.org/wiki/Chopsticks.

[18] Spaghetti is hard to control because it mostly fractures into three segments with arbitrary length. The middle segment will spring off and collide with other spaghetti to cause many unwanted noises. This problem was most serious halfway through fracturing the bundle of spaghetti. As a result, the data for spaghetti appeared more scattered than those for the chopstick in Fig. 3. In addition, spaghetti lacks the abundant and weak mode-I crackling sound when bamboo fibers detach from each other. This perhaps explains why the b value for spaghetti in Fig. 3(d) is smaller than that for the chopstick in Fig. 3(a) (https://www.youtube.com/watch?v=ADD7QlQoFFI); B. Audoly and S. Neukirch, Phys. Rev. Lett. **95**, 095505 (2005).

[19] B. Gutenberg and C. F. Richter, Bull. Seismol. Soc. Am. **34**, 185 (1944); *Seismicity of the Earth and Associated Phenomena*, 2nd ed. (Princeton University Press, Princeton, 1954).

[20] D. Schorlemmer, S. Wiemer, and M. Wyss, Nature (London) **437**, 539 (2005) concluded that the b value could vary for different styles of faulting.

[21] F. Omori, J. Coll. Sci. Imp. Univ. Tokyo **7**, 111 (1895).

[22] M. Hamdache, J. A. Pelaez, and A. Talbi, *Earthquake Research and Analysis—New Advances in Seismology*, edited by S. D'Amico (InTech, Rijeka, 2013), Chap. 3.

[23] A. Helmstetter and D. Sornette, Geophys. Res. Lett. **30**, 2069 (2003).

[24] M. Båth, Tectonophysics **2**, 483 (1965).

[25] M. Minozzi, G. Caldarelli, L. Pietronero, and S. Zapperi, Eur. Phys. J. B **36**, 203 (2003).

[26] https://www.youtube.com/watch?v=D_W_RpMKNPI.

[27] M. H. Chou, W. C. Shen, Y. P. Wang, S. H. Hung, and T. M. Hong, Phys. Rev. Lett. **112**, 034302 (2014).

[28] S. T. Tsai, C. D. Chang, C. H. Chang, M. X. Tsai, N. J. Hsu, and T. M. Hong, Phys. Rev. E **92**, 062925 (2015).

[29] H. Akaike, in *Proceedings of the 2nd International Symposium on Information Theory*, edited by B. N. Petrov and F. Csaki (Akademial Kiado, Budapest, 1973), pp. 267–281; B. N. Petrov and F. Csaki*IEEE Trans. Autom. Control* ***19****, 716 (1974)*; B. N. Petrov and F. Csaki*A Celebration of Statistics*, edited by A. C. Atkinson and S. E. Fienberg (Springer, Berlin, 1985), pp. 1–24.

[30] P. Bak, C. Tang, and K. Wiesenfeld, Phys. Rev. Lett. **59**, 381 (1987); C. Tang and P. Bak, *ibid.* **60**, 2347 (1988).

[31] K. Christensen, L. Danon, T. Scanlon, and P. Bak, Proc. Natl. Acad. Sci. U.S.A. **99**, 2509 (2002).

[32] A. Carpinteri and N. Pugno, Nature (London) **4**, 421 (2005).